

**Enhanced Image Resolution in photonic crystal structure
by modification of the surface structure**

A Dissertation submitted towards the partial fulfillment of the requirement for the award of
degree of

**Master of Technology in
Nano science and Technology**

Submitted by

Ashwini Agarwal

2k14/NST/02

Under the supervision of

Dr. Yogita Kalra

Assistant Professor



Department of Applied Physics

Delhi Technological University

(Formerly Delhi College of Engineering)

JUNE 2016



CERTIFICATE

I hereby certify that the work which is being presented in the M.Tech thesis entitled “**Enhanced Image Resolution in photonic crystal structure by modification of the surface structure**”, in partial fulfillment of the requirements for the award of the **Master of Technology in Nano Science & Technology** submitted to the Department of Applied Physics, Delhi Technological University, Delhi-110042 is an authentic record of my own work carried out during the period July 2015 to June 2016 under the supervision of **Dr. Yogita Kalra**, Assistant Professor, Department of Applied Physics .

The matter presented in this report has not been submitted by me for the award of any other degree or diploma elsewhere.

Signature of the Candidate

This is to certify that the above statement made by the candidate is correct to the best of my knowledge.

Signature of the Supervisor

Dr. Yogita Kalra

Assistant Professor

Department of Applied Physics

Delhi Technological University

Delhi-110042

Signature of the HOD

Prof. S. C. Sharma

Head of the department

Department of Applied Physics

Delhi Technological university

Delhi-110042

DECLARATION

I hereby declare that all the information in this document has been obtained and resented in accordance with academic rules and ethical conduct. This report is my own, unaided work. I have fully cited and referenced all material and results that are not original to this work. It is being submitted for degree of Master of Technology in **Nano Science and Technology at Delhi Technological University**. It has not been submitted for any degree or examination in any other university.

Date:

ASHWINI AGARWAL

Place

MTECH (NST)

2k14/NST/02

ACKNOWLEDGEMENT

I take this opportunity as a privilege to thank all individuals without whose support and guidance. I could not have completed my project successfully in this stipulated period of time.

First and foremost, I would like to express my deepest gratitude to my supervisor **Dr. Yogita Kalra , Asst. Professor, Department of Applied Physics** for her invaluable support, guidance, motivation and encouragement throughout the period this work was carried out. I am grateful to her for closely monitoring my progress and providing me with timely and important advice, their valued suggestions and inputs during the course of the project work.

I am deeply grateful to **prof. S.C. Sharma** for his support and encouragement in carrying out this project.

I also wish to express my heart full thanks to the classmates as well as staff at department of applied physics of Delhi Technological University for their goodwill and support that helped me a lot successful completion of this project.

Finally, I want to thank my parents, brother and friends for always believing in my abilities and for always showering their invaluable love and support.

ASHWINI AGARWAL

MTECH (NST)

2K14/NST/02

TABLE OF CONTENTS

ACKNOWLEDGEMENT

TABLE OF CONTENTS

ABSTRACT

LIST OF PUBLICATIONS

LIST OF TABLES

LIST OF FIGURES

Chapter1 Introduction

1.1 Thesis Approach.....	1
1.2 Thesis Objective.....	1
1.3 Thesis Organization.....	2

Chapter 2 Introduction of Photonic Crystal

2.1Introduction.....	3
2.2Mathematical analysis and Computational Techniques.....	7
2.3 Plane wave Expansion Method.....	9
2.4 Finite Difference Time Domain Method.....	10
2.5 Defects in Photonic Crystals.....	11
2.6 Application of Photonic Crystal.....	13

Chapter 3 Theory of Image Processing

3.1 Imaging.....	16
3.2 Refraction.....	16
3.3 Negative Refraction.....	17
3.4 Negative Refraction Using PhCs.....	20
3.5 Negative Effective Index.....	20
3.6 Sub Wavelength Imaging.....	23
3.7 Equal frequency contour.....	24

Chapter 4 Enhanced Image Resolution in Photonic Crystal Structure by Modification of The Surface Structure

4.1 Introduction.....	26
4.2 design Parameter.....	27
4.3 Numerical Analysis.....	28
4.4 Application of Proposed Structure As a Sensor.....	29
4.5 Conclusion.....	34

Chapter 5 Conclusion and Future Scope

5.1 Conclusion.....	35
5.2 Future Scope.....	35
References.....	37

ABSTRACT

Photonic crystals are inhomogeneous dielectric media with periodic variation of the refractive index. A photonic crystal gives us new tools for the manipulation of photons and thus has received great interests in a variety of fields. Photonic crystals also have applications in imaging. A number of imaging principles were demonstrated. In this thesis we focused, enhance the image resolution of photonic crystal by modification the surface structure and used the structure as a sensor. We utilize the superlens behaviour of the photonic crystal (PhC) structure composed of hexagonal lattice arrangement of air holes of radius ' $r = 0.35a$ ', where ' a ' is the lattice constant, in a dielectric medium of permittivity $\epsilon = 12$. The equal frequency contour (EFC) analysis done using plane wave expansion method shows that the structure exhibits an effective isotropic refractive index, $n_{\text{eff}} = -1$ at a normalized frequency of $\omega = 0.2908(2\pi c/a)$ for TM polarization, located in the second band. At $\omega = 0.2908(2\pi c/a)$ for TM polarization, the considered PhC structure behaves as a superlens, as analyzed using the finite difference time domain (FDTD) method.

Key words: Photonic crystal, superlens Behaviour, Equal Frequency Contour (EFC), Effective refractive index, TM polarization, Finite difference time domain (FDTD) method.

List of Publications

1. Ashwini Agarwal, Preeti Rani, Yogita Kalra, and R.K Sinha, “Enhanced Image Resolution in photonic crystal structure by modification of the surface structure and its application as a sensor”, in International Conference SPIE optics + photonics 2016 (Photonic Fiber and Crystal Devices: Advances in Materials and Innovations in Device Applications X), to be held in San Diego, California, USA from 28 August - 1 September 2016 having paper number 9958-16

List of Tables

Table 1 Filtration of Blood Constituents in top layer of air holes.

Table 2 Filtration of Blood Constituents in bottom layer of air holes.

List of Figures

Figure 2.1. Schematic illustrations of photonic crystals (a) 1D (b) 2D and (c) 3D

Figure 2.2 Structure of (a) dielectric rods in air and (b) air holes in dielectric region

Figure 2.3. Structure of 3D woodpile photonic crystals

Figure 2.4 Photonic Band Gap diagram of a 1D DBR with $d/a = 0.8$, $\epsilon = 12.25$

Figure 2.5 5x5 supercell with Point defect

Figure 2.6 point defect with increasing radii

Figure 2.7 Some examples of waveguides in 2D photonic crystals: (a) W1 waveguide (waveguide having a width of one pore row) consisting of a row of missing pores, (b) W1 waveguide consisting of a row of pores with smaller diameter, (c) coupled-cavity waveguide and (d) W3 waveguide (three pore-rows wide).

Figure 2.8 Applications of photonic crystals

Figure 3.1 Phenomenon of refraction

Figure 3.2 (a) Schematic depiction of the negative refraction at an interface between a positive medium and a negative medium. The energy flow and the phase vectors are in opposite directions in the NRM. (b) The negative refraction effect through a prism. (c) Flat slab of NRM that can focus a point source from one side of the slab to the other side.

Figure 3.3 Principle of refraction by Snell's law

Figure 3.4 Negative and positive refraction

Figure 3.5 Imaging by a flat slab of thickness T of negative index material with $n_1 = -1$ and surrounded by vacuum. A point source P is positioned at a distance D from the left surface of the slab. A "perfect" image of the source can be observed at the point P' , located at a distance $T-D$ from the right surface of the slab.

Figure 3.6 Equal frequency surfaces (EFSs) of a homogenous dielectric medium

Figure 4.1 PhC structure composed of air holes of radius ' $r = 0.35a$ ' in silicon

Figure 4.2 (a) band gap of PhC structure composed of air holes of radius ' $r = 0.35a$ ' with light line for TM polarization. (b) Several equal frequency contours of the second band at the TM mode in the first Brillouin zone

Figure 4.3 (a) Band gap of PhC structure composed of air holes of radius ' $r = 0.35a$ ' with light line for TM polarization (b) Several equal frequency contours of the second band at the TE mode in the first Brillouin zone

Figure 4.4 Image processing and field distribution across image center along X-direction

Figure 4.5(a) modified photonic crystal structure with radius ' $r = 0.35a$ ' and ' $r_1 = 0.41a$ '; (b) radius of outer semicircle and semi circle is r_1 and distance between two semicircles is d

Figure-4.6 Image processing and field distribution across image center along X- direction of modified photonic crystal structure

Figure 4.7 Peak graphs of all blood constituents filled in top layer

Figure 4.8 Intensity curve of different type of blood constituents, intensity peak increased when refractive index increased.

Figure 4.9 FWHM curve of different type of blood constituents, FWHM decreased when refractive index increased

CHAPTER 1

INTRODUCTION

1.1 Thesis Approach

This Thesis proposes a design of 2D photonic crystal structure (PhC) which consists of air holes in silicon. Image resolution has been enhanced in the PhC structure by introducing the defects at the surface of the proposed structure. Negative refraction phenomenon has been used to calculate the negative effective index ($n_{\text{eff}}^{\text{neg}}$) at a particular frequency. This frequency has been calculated using the photonic band gap and equal frequency contour. Materials with negative effective index behave like superlens at this frequency. The structure has been designed and analyzed using Bandsolve and full wave module of commercially available R-soft software.

1.2 Thesis objective

The main objective of the thesis is mentioned below:

- To explore the possibility of using photonic crystal as negative index material at a particular frequency.
- To explore and analyze various ways to enhance the image resolution in photonic crystal structures and study different types of photonic crystal structures which can be used for analyzing the image resolution.
- To design the photonic crystal structure of hexagonal arrangement of air holes in silicon with the introduction of defect in top and bottom layer of the surface of PhC structure to enhance the image resolution.
- To design the PhC sensor using the concept of image resolution.

1.3 Thesis organization

This thesis has been organized into five chapters.

Chapter 1 deals with the introduction and objective of the thesis.

Chapter 2 describes the literature review, consisting of photonic crystal, their historical background, basic properties and their applications.

Chapter 3 is regarding the theory of image processing, refraction, negative refraction, negative refractive index, imaging and sub wavelength imaging.

Chapter 4 deals with the designed PhC structure for Enhanced image resolution and the superlens behavior established by the proposed structure..

Chapter 5 includes conclusion and future scope regarding the image resolution in PhC structures.

CHAPTER 2

INTRODUCTION OF PHOTONIC CRYSTAL

2.1 Introduction

Photonic crystal (PhC) is one of the most promising platforms for optical information processing as it enables compact and efficient photonic devices and also their large scale integration onchip. These are the structures with periodic dielectric modulation in the order of the wavelength of light [1, 2]. Because of this periodicity, their study is analogous to the study of semiconductors in solid-state physics. The periodicity of the electronic potential in semiconductors, which is due to the regular arrangement of atoms in a lattice, gives rise to the electronic bandgaps, which are forbidden energy bands[1,2] for electrons. Similarly, the periodicity of the refractive index gives rise to photonic bandgaps (PBGs), forbidden energy bands for photons.

Electromagnetic wave propagation in dielectric periodic media was first studied by Lord Rayleigh in 1888. These structures are photonic crystals which have a photonic band gap that prohibits the light propagation through the planes. Although PhCs have been studied in one form or another since 1887, the term “Photonic Crystal” was first used over 100 years later, after Yablonovitch and John published two milestone papers on PhCs in 1988. Before that Lord Rayleigh started his study in 1888, by showing that such systems have a 1D Photonic Band Gap, a spectral range of large reflectivity, known as a stop-band. Further, 1D PhCs in the form of periodic multi-layers dielectric stacks (such as the Bragg mirror) has been studied extensively. Today, such structures are being used in a diverse range of applications such as reflective coatings for enhancing the efficiency of Light Emitting Diodes (LEDs) and highly reflective mirrors in certain laser cavities.

In 1987, Yablonovitch and John proposed 2D PhCs and 3D PhCs, which had a periodic dielectric structure in two dimensions and three dimensions, respectively. The periodic dielectric structures exhibit a PBG. Both of their proposals were concerned with higher dimensional (2D or 3D) periodic optical structures. Yablonovitch's main motivation was to engineer the photonic density of states, in order to control the spontaneous emission of materials that are embedded within the PhC. In the similar way, John's idea was to affect the localization and control of light inside the

periodic PhC structure. Since 1987, There has been extensive research in the area of PhCs. By 1991, Yablonovitch has demonstrated the first 3D Photonic Band Gap in the microwave regime. In 1996, Thomas Krauss made the first demonstration of 2D PhC at optical wavelengths. This opened the modern way of fabricating PhCs in semiconductor materials by the methods used in the semiconductor industry. Although such techniques are still to mature into commercial applications, 2D PhCs have found commercial use in the form of Photonic Crystal Fibers (PCFs) and optical components. Since 1998, the 2D PhCs based optical components such as optical filters [3, 4], multiplexers [5], demultiplexers [6], switches [7], directional couplers [8], power dividers/splitters [9], sensors [10, 11] etc. has been realized.

The PhCs are composed of periodic dielectric, metallo-dielectric or superconductor nanostructure that affect electromagnetic wave propagation in the same way as the periodic potential in a semiconductor crystal affects the motion of electrons. Photonic crystals exhibit regularly repeating regions of high or low dielectric constants. The periodicity of the photonic crystal structure must be around half the wavelength of the electromagnetic waves to be diffracted. Depending on the periodicity of the dielectric constant along layers, plane & axes, they are one dimensional (1D), two dimensional (2D) and three dimensional (3D) photonic crystal structures as shown in figure 2.1.

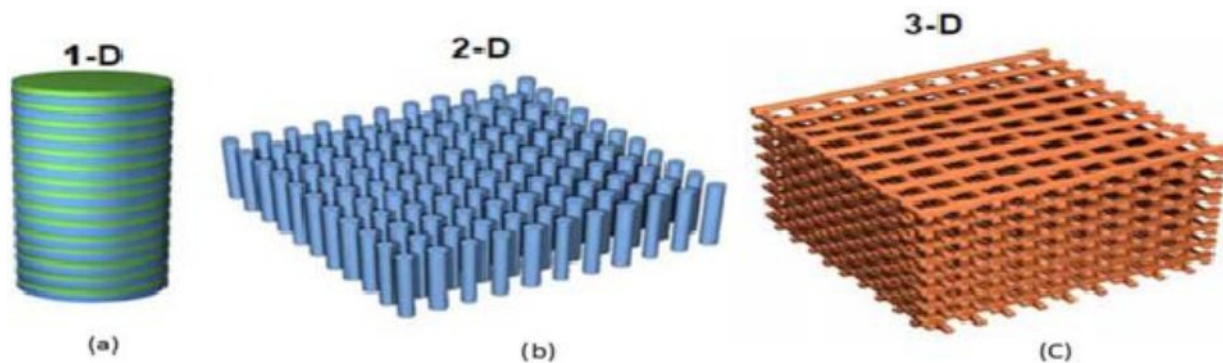


Figure 2.1. Schematic illustrations of photonic crystals (a) 1D (b) 2D and (c) 3D

(Source: www.intechopen.com)

2.1.1 One Dimensional PhCs

In 1-DPhC, the periodic modulation of the refractive index occurs only in one direction, while the refractive index variations are uniform for other two directions of the structure. The Photonic Band Gap appears in the direction of periodicity at different values of refractive index contrast. In other words, there is no threshold for dielectric contrast for the appearance of a Photonic Band Gap. For smaller values of index contrast, the width of the Photonic Band Gap appears very small and vice versa. However, the Photonic Band Gaps open up as soon as the refractive index contrast is greater than one ($n_1/n_2 > 1$), where n_1 and n_2 are the refractive index of the dielectric materials. A defect can be introduced in 1-DPhC, by making one of the layers having slightly different refractive index or width than the rest. The defect mode is then localized in one direction however it is extended to other two directions. An example for such 1-DPhC is the well known dielectric Bragg mirror consisting of alternative layers with low and high refractive indices, as shown in Figure 2.1(a).

The wavelength and reflection properties in 1-D PhC are used in many applications including high efficiency mirrors [12, 13], optical filters [14, 15, and 16], waveguides and lasers [17]. Such structures are widely used in anti-reflecting coatings which decrease the reflectance from the surface and used to improve the quality of the lenses, prisms and other optical components.

2.1.2 Two Dimensional PhCs

PhC structures that are periodic in two different directions and homogeneous in third direction are called 2-D PhC which is shown in Figure 2.1 (b). In most of the 2-DPhCs, the Photonic Band Gap occurs when the lattice has sufficiently large index contrast. If the refractive index contrast between the rods and the background medium is sufficiently large, 2-D Photonic Band Gap occurs in the plane of periodicity perpendicular to the rod axis. Generally, 2-DPhCs consist of dielectric rods in air host (high dielectric pillars embedded in low dielectric medium) or air holes in a dielectric region (low dielectric rods in a connected higher dielectric lattice) as shown in Figures 2.2(a) and 2.2(b). The dielectric rods in air host give Photonic Band Gap for the Transverse Magnetic (TM) mode where the E field is polarized perpendicular to the plane of periodicity. The air holes in a dielectric region give (Transverse Electric) TE modes where H field is polarized perpendicular to the plane of periodicity.

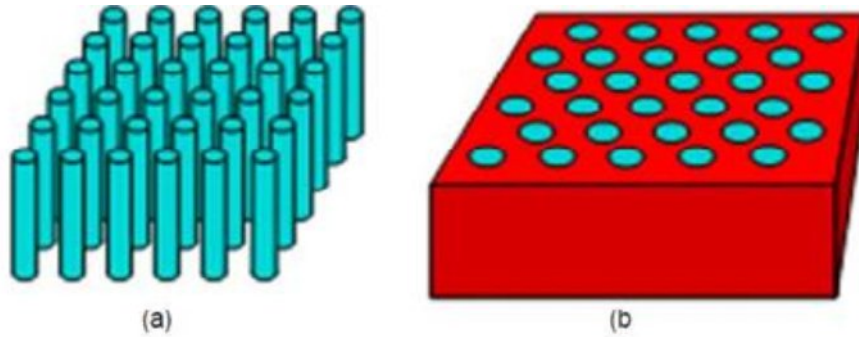


Figure 2.2 Structure of (a) dielectric rods in air and (b) air holes in dielectric region

(Source: www.intechopen.com)

2.1.3 Three Dimensional PhCs

A 3DPhC is a dielectric structure which has periodic permittivity modulation along three different axes, provided the condition of sufficiently high dielectric contrast and suitable periodicity; a Photonic Band Gap appears in all directions. Such 3D Photonic Band Gaps, unlike the 1D and 2D ones, can reflect light incident from any direction. In other words, a 3D Photonic Band Gap material behaves as an omnidirectional high reflector. As an example, Figure 2.3 depicts the 3D woodpile structure. Due to the challenges in high-quality structures fabrication at optical wavelengths, early PhCs performed at microwave and mid-infrared frequencies [19, 20]. With the improvement of fabrication and materials processing methods, smaller structures have become feasible, and in 1999 the first 3DPhC with a Photonic Band Gap at telecommunications frequencies [21, 22] was reported. Since then, various lattice geometries have been reported operating at similar frequencies [23, 24]. The introduction of intentional defects in 3D PhCs are difficult as compared to 2D PhCs due to the fabrication hurdles and more complex geometry requirements.

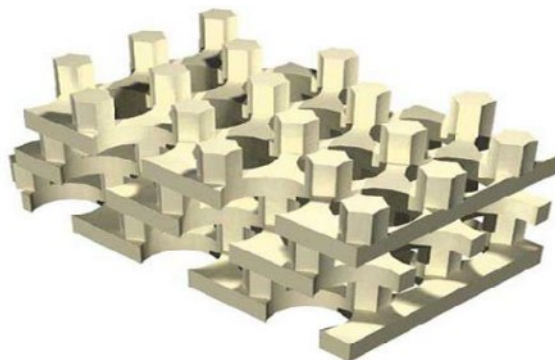


Figure 2.3. Structure of 3D woodpile photonic crystals

(Source: <http://ab-initio.mit.edu/photons/3d-crystal.html>)

2.2 Mathematical analysis and Computational Techniques

The fundamental studies of the propagation of light in general photonic structures can be done using the four macroscopic Maxwell equations:

$$\nabla \cdot \mathbf{D} = \rho \quad \nabla \times \mathbf{E} = -\frac{\partial \mathbf{B}}{\partial t} \quad (2.1)$$

$$\nabla \cdot \mathbf{B} = 0 \quad \nabla \times \mathbf{H} = \mathbf{J} + \frac{\partial \mathbf{D}}{\partial t} \quad (2.2)$$

Here, \mathbf{E} and \mathbf{H} is the macroscopic electric and magnetic fields respectively, \mathbf{D} and \mathbf{B} are the displacement current and magnetic field intensity and \mathbf{J} and ρ are the free current density and charge density [24, 25]. All parameters depend on time t , space vector \mathbf{r} and the frequency of light ω . For linear, isotropic and lossless material, $\mathbf{J}=0$ and $\rho=0$. With this simplification, we can relate the field \mathbf{E} to \mathbf{D} by the relation $\mathbf{D} = \epsilon(\mathbf{r}) \mathbf{E}$, with the dielectric function $\epsilon(\mathbf{r})$. For non magnetic dielectric materials [25], magnetic permeability $\mu=1$, so \mathbf{H} and \mathbf{B} are related by the relation, $\mathbf{B} = \mathbf{H}$. The Maxwell equations for a nonmagnetic dielectric medium are

$$\nabla \cdot \mathbf{D} = 0 \quad \nabla \times \mathbf{E} = -\frac{\partial \mathbf{B}}{\partial t} \quad (2.3)$$

$$\nabla \cdot \mathbf{B} = 0 \quad \nabla \times \mathbf{H} = \frac{\partial \mathbf{D}}{\partial t} \quad (2.4)$$

Where, c is the speed of light and the dielectric function $\epsilon(\mathbf{r})$. These four equations determine the interaction between light and dielectric materials.

Both fields, the electric and the magnetic field, will be complicated functions of space and time. Since the fields in Maxwell's equations are linear functions, the time- and space-dependency of the fields can be separated by expanding each field into its (time-harmonic) Fourier modes. The magnetic and electric field thus becomes

$$\mathbf{E}(\mathbf{r}, t) = \sum_{\mathbf{k}} \mathbf{E}_{\mathbf{k}}(\mathbf{r}) e^{-i\omega_{\mathbf{k}} t} \quad (2.5)$$

$$\nabla \cdot \epsilon \nabla \phi = -\rho \quad (2.6)$$

This implies the absence of (electric or magnetic) point sources. Hence

$$\nabla \cdot \epsilon \nabla \phi = 0 \quad (2.7)$$

This implies that no (electric or magnetic) point sources are present in the medium. We can use two curl equations to get

$$\nabla \times \nabla \times \mathbf{E} = -\mu \nabla \times \mathbf{H} \quad (2.8)$$

$$\nabla \times \nabla \times \mathbf{H} = \frac{1}{\mu} \nabla \times \nabla \times \mathbf{E} \quad (2.9)$$

These equations can be decoupled into a closed equation of $\mathbf{H}(\mathbf{r})$. From these equations, we can get the following equation

$$\nabla \times \frac{1}{\mu} \nabla \times \mathbf{H} = \frac{1}{\mu} \nabla \times \nabla \times \mathbf{E} \quad (2.10)$$

Which can be generally expressed as an Eigen value problem $\Phi_h \mathbf{H}(\mathbf{r}) = \left(\frac{1}{\mu}\right) \nabla \times \nabla \times \mathbf{E}$ with the

Hermitian operator $\Phi_h = \nabla \times \frac{1}{\mu} \nabla \times$ When $\mathbf{H}(\mathbf{r})$ is known, the electric field $\mathbf{E}(\mathbf{r})$ can be

calculated as:

$$\mathbf{E}(\mathbf{r}) = \frac{1}{\mu} \nabla \times \mathbf{H}(\mathbf{r}) \quad (2.11)$$

A similar equation in magnetic field $\mathbf{H}(\mathbf{r})$ can be observed as

$$\mathbf{H}(\mathbf{r}) = \frac{1}{\mu} \nabla \times \mathbf{E}(\mathbf{r}) \quad (2.12)$$

To analyze the master equation and light propagation in PhC structure various numerical techniques are used such as

- Plane wave Expansion Method [25, 26]
- Finite Difference Time domain Method [24]
- Finite Element Method

These methods are used to solve the frequency of the photonic crystal for each value of propagation direction given by wave vector.

2.3 Plane wave Expansion Method

The plane wave expansion method is a classical method to calculate band structure in semiconductors that can take advantage of the periodicity of the lattice. Because of translational symmetry fields can be expanded in terms of Bloch- vectors. The dielectric function periodicity permits obtaining its Fourier transformation (in the wave vector space) only in terms of reciprocal lattice vectors. Fourier transformation is now a discrete summation and the problem is reduced to diagonalize a matrix. Apart from all the assumptions explained before, the PWM requires a real dielectric function; this means that the composing material of our photonic crystal must be lossless.

The method can be used to calculate the band structure using an Eigenformulation of the Maxwell's equations, and thus solving the Eigen frequencies for each of the propagation directions of the wave vectors. Electric field strength can also be calculated by the using of problem of the Eigen vectors. Figure 2.4 shown below, corresponds to the band-structure of a 1D distributed Bragg reflector (DBR) with air-core interleaved with a dielectric material of relative permittivity 12.25, and a lattice period to air-core thickness ratio (d/a) of 0.8, is solved using 101 planewaves over the first irreducible Brillouin Zone.

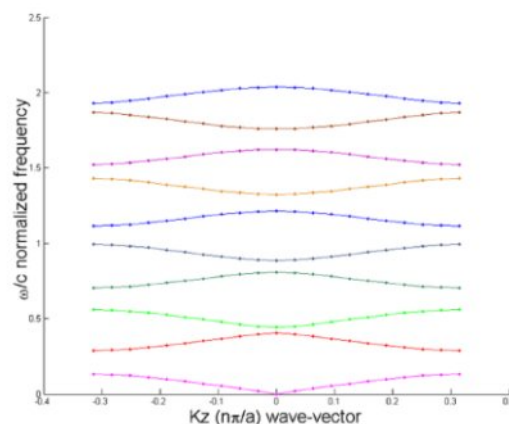


Figure 2.4 Photonic Band Gap diagram of a 1D DBR with $d/a = 0.8$, $\epsilon = 12.25$

(Source: www.thelivingmoon.com)

This technique is used for solving band structures of different photonic crystals. Equations are formulated into Eigen value (ω^2/c^2) problem.

For simplicity we take the E-polarization:

$$\nabla \cdot \left(\frac{1}{\epsilon} \nabla \phi \right) + \left(\frac{\omega^2}{c^2} - \frac{1}{\epsilon} \right) \phi = 0 \quad (2.13)$$

$$\left(\frac{\partial}{\partial x} \frac{1}{\epsilon} \frac{\partial}{\partial x} + \frac{\partial}{\partial y} \frac{1}{\epsilon} \frac{\partial}{\partial y} \right) \phi + \left(\frac{\omega^2}{c^2} - \frac{1}{\epsilon} \right) \phi = 0 \quad (2.14)$$

Using Bloch Theorem we have:

$$\nabla \cdot \left(\frac{1}{\epsilon} \nabla \phi \right) + \left(\frac{\omega^2}{c^2} - \frac{1}{\epsilon} \right) \phi = 0 \quad (2.15)$$

Hence,

$$\nabla \cdot \left(\frac{1}{\epsilon} \nabla \phi \right) + \left(\frac{\omega^2}{c^2} - \frac{1}{\epsilon} \right) \phi = 0 \quad (2.16)$$

2.4 Finite Difference Time Domain Method (FDTD):

Finite-difference time-domain (FDTD) is one of the primary available computational electrodynamics modeling techniques. The FDTD method [26] belongs in the general class of grid-based differential time-domain numerical modeling methods. The time-dependent Maxwell's equation in partial differential form is discretised using central difference approximations to the space and the time partial derivatives. The resulting finite difference equations are solved in either software or hardware. The electric Field vector components in a volume of space are solved at a given instant in time and the process is repeated over and over again until the desired transient or steady-state electromagnetic field behavior is fully evolved. The electric and magnetic fields are distributed in an alternating manner, such that a magnetic field vector lies in between two electric field vectors [24, 27]. A given photonic structure is then constructed according the given values of permittivity and permeability to each electric field component and magnetic field component, respectively.

The advantage of these methods are that there are no conditions over scattering, shape, absorption effect can be taken into account by introducing imaginary values in the dielectric constant. In 1992 pendry et.al proposed transfer matrix method based on finite difference frequency method (FDFD) to compute the transmission and reflectance spectra of PhC.

2.5 Defects In Photonic Crystals

Defect [28] engineering is one of the design criteria to control the propagation of light in PhC structures. The modes that have frequencies inside the band gap are not allowed to propagate in the parent lattice. On perturbing a lattice at a single site may permit the existence of a localized point defect mode or a set of modes that have frequencies within the band gap range. The defect mode may act as a surface emitter or in plane emitter depending on the number of layer of 2d photonic crystal that surrounding defects. Light can also be trapped by combining different point defects in row or a column thus lead to the formation of line defect waveguide. In photonic we study two types of defects as mentioned below:

2.5.1. Point Defect

A point defect [29] can be introduced in a two dimensional photonic crystals by either removing one rod or by increasing the radius of the rod. Due to point defect overall dielectric constant decrease and the latter would increase the overall dielectric constant. According to the principle, if the defect caused by the average dielectric constant to decrease, then the eigenfrequencies would shift to higher frequencies, causing one or more bands from the bands near bottom of the band gap to shift in to the band gap. On the other hand, if the defect caused the average dielectric constant to increase, then the eigenfrequencies would shift to lower frequencies, causing one or more bands from the bands near top of the band gap to shift into the band gap. Thus one or more localized modes can be achieved by introducing a point defect.

A point defect can be created by removing one rod from the center of the 5 x5 supercell as shown in figure 2.5. Due to removal of a rod causes the average dielectric constant of the lattice to decrease. The defect modes are discrete bands, which are constant for all k vectors in the irreducible Brillouin zone [30], if the mode is localized in the band gap, it is evanescent.

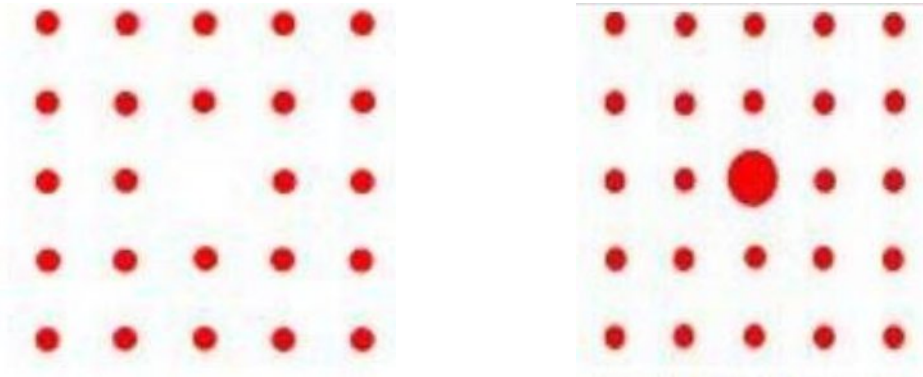


Figure 2.5 5x5 supercell with Point defect **Figure 2.6** point defect with increasing radii

The defect mode cannot propagate to the rest of crystal. This localized mode behaves as a cavity surrounded by reflecting walls. Near the localized field distribution degenerate bands are formed. Displacement field intensity is very high, localized at the point defect. Therefore the defect rod behaves as a cavity surrounded by reflecting walls. Light cannot escape from the cavity and this concept is very useful in manufacturing resonant cavities for lasers.

A point defect was also created by increasing the radius of the centre rod in the 5 x 5 supercell as shown in figure 2.6. The average dielectric constant increased after the defect was created, causing the bands above the band gap to shift into the band gap. This structure can be used as a multi frequency filter or as a resonant cavity [31] for modes of normalized frequencies. Point defect based micro cavity is very small in size and has an extremely narrow spectral width and high Q values. It acts as a high-Q filter [32], or a centre of energy transfer. The Q value of the resonant cavity cannot be calculated using plane wave expansion method. FDTD [24] simulation must be done in order to find the Q value of the resonant cavity.

2.5.2. Linear Defect: waveguide

A line defect [33] is introduced into the 2D photonic crystal lattice by changing the radius of entire line or removing completely, some defect states are created. Light cannot propagate in the photonic crystal at the frequency of linear defect mode. The line defect act as a waveguide [34], figure 2.7 shows some example of linear waveguide in 2-D photonic crystal.

The introduction of a line defect induces a symmetry breaking. The translation symmetry exists only in the direction parallel to the defect. Therefore, the new Brillouin zone [30] is 1D, and the band structure of the 2D photonic crystal has to be projected onto the k-path Γ (0)–J (π/a) of the

new Brillouin zone. The band structure for TE modes of a W1 waveguide consisting of a row of missing pores in the Γ -K direction

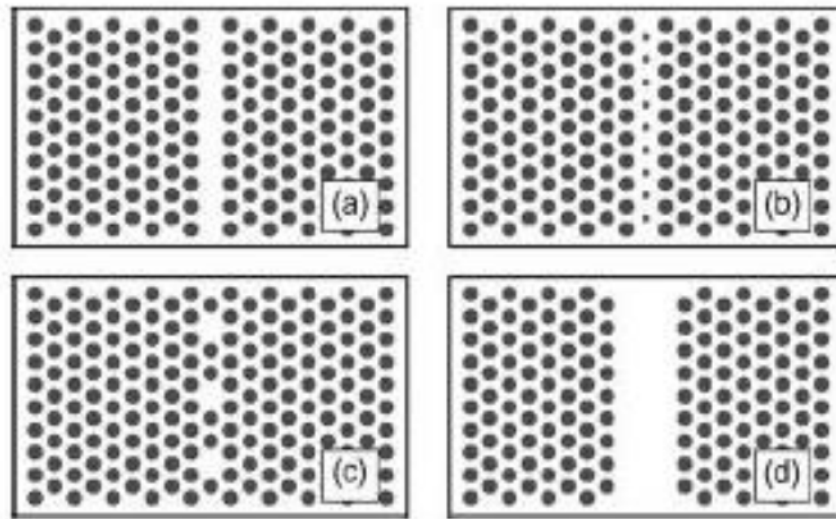


Figure 2.7 Some examples of waveguides in 2D photonic crystals: (a) W1 waveguide (waveguide having a width of one pore row) consisting of a row of missing pores, (b) W1 waveguide consisting of a row of pores with smaller diameter, (c) coupled-cavity waveguide and (d) W3 waveguide (three pore-rows wide). Source: [33]

2.6 Applications of Photonic Crystals

Photonic crystals are attractive optical materials for controlling and manipulating the flow of light. One dimensional photonic crystal are already used in the form of thin-film optics with applications ranging from low and high reflection coatings on lenses and mirrors, colour changing paints and inks. Higher dimensional photonic crystals are of great interest for both fundamental and applied research, and the two dimensional are beginning to find commercial applications. K.Inoue have summarizes the relation of PhCs with other optics and various applications now being developed as shown in figure 2.8. Considering that PhCs exhibit their functionalities by multi diffraction and multi scattering, a PhC can be said to be a kind of hologram in a broad sense. A novelty of PhCs, compared with conventional holograms, is the precise design method, namely the photonic band calculation, which is very effective for estimating their functionalities and performance.

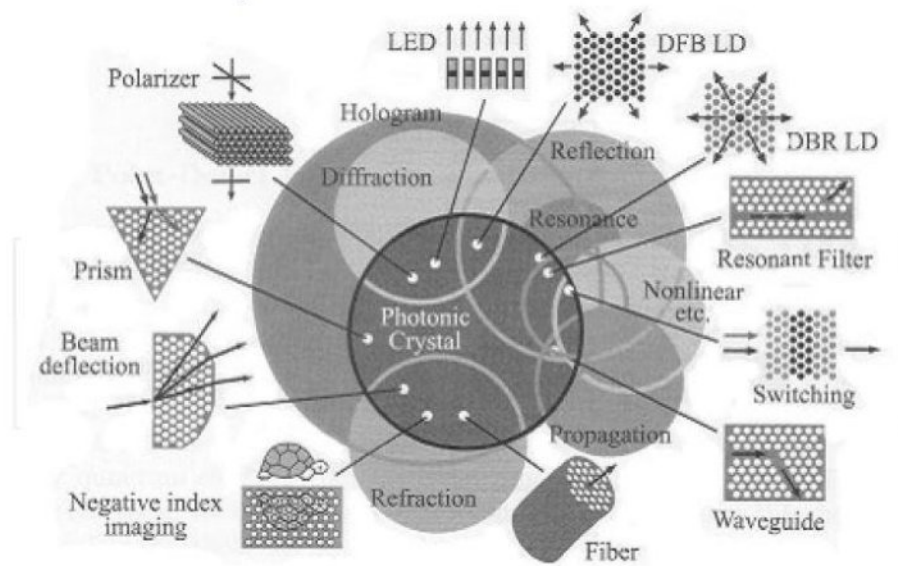


Figure 2.8 Applications of photonic crystals

(Source: K. Inoue et al. 2004)

The field of photonic crystal is very appealing due to the numerous exciting applications. Fabrication of integrated circuits in which photons replacing electrons as the information carrier is one of the most sought after applications for photonic crystals. In this direction, waveguide based on 2D photonic crystals is already made by researchers and studies are ongoing to improve the quality of such structures.

Photonic crystals even without a complete photonic band gap can be designed to obtain super collimators and super-lenses. Two photons that impinge a photonic crystal with the same angle but a slightly different energy, may find equi-frequency surfaces with a very different curvature. As a consequence their propagation angles would be very dissimilar. This is known as super prism effect and could be applied to the fabrication of small integrated multiplexers. Recently it has been shown that photonic crystals have the ability to create negative refraction of light. Photonic crystals that exhibit all- angle negative refraction can be used to obtain super-lenses that could potentially overcome the diffraction limit inherent in conventional lenses.

Although there is a large amount of research going on waveguide based on total internal reflection, photonic crystals have some definite advantages. For example sharp bends in a photonic crystal based waveguide do not present losses as high as those on total internal reflection. The electric field patterns in different PhC wave guide configuration. Here the mode is completely confined inside the guide and travels smoothly around the bend even if radius of

curvature of the bend is of the order of wavelength of light. In the case of wide angle splitter the fields are split equally into output waveguides.

In order to obtain integrated circuits that could perform logical operations a photonic transistor would be necessary. For this a system based on two-level atoms having population inversion near the photonic band gap edge has been reported. The spontaneous emission of light was often considered as intrinsic physical phenomenon difficult to control. This phenomenon can, in principle, be inhibited by using photonic crystals, has also been reported in recent years. Since spontaneous emission of light significantly affects the efficiency of semiconductor lasers, solar cells etc structure which can control it will pave the way for the making of efficient energy saving devices.

CHAPTER 3

THEORY OF IMAGE PROCESSING

3.1 Imaging

Imaging is the process of reproduction of the visual attributes of an object using a certain instrument (generally a lens system). Various types of methodologies and technologies are used for imaging such as Chemical imaging, digital imaging, disk imaging, radar imaging, optical imaging etc. The conventional imaging techniques make use of lenses which collect light emerging from an object and focus it to form a sharp image. But conventional lenses suffer from a drawback called diffraction limit [35] due to which they are unable to produce a well-resolved image of a sub wavelength (smaller than operating wavelength) object. This restriction can be overcome by a negative refractive index metamaterials lens also called a perfect lens or a superlens. Negative refractive index metamaterials are those artificially designed materials which have negative ϵ and negative μ at particular wavelength. Consequently, these materials have negative refractive index and exhibit negative refraction. To behave as a perfect lens, the refractive index of metamaterials should be negative of the refractive index of the surrounding medium. The sub wavelength imaging technology can revolutionize Biomedical Science by providing a facility to observe extremely small objects such as viruses, DNA, RNA or even protein molecules.

3.2 Refraction

Refraction [36] is the phenomenon in which change in direction of propagation of a wave due to a change in its transmission medium as shown in figure 3.1. When a beam of light encounters another transparent medium, a part of light gets reflected [36] back into the first medium while the rest enters the other. The direction of propagation of an obliquely incident ray of light that enters the other medium, changes at the interface of the two media. Snell experimentally obtained the following laws of refraction:

- The incident ray, the refracted ray and the normal to the interface at the point of incidence, all lie in the same plane.

- The ratio of the sine of angle of refraction is constant. The angles of incidence (i) and refraction(r) are the angles that the incident and its refracted ray make with the normal, respectively. We have

$$\frac{\sin i}{\sin r} = n_{21} \quad (3.1)$$

Where, n_{21} is a constant, called the refractive index of the second medium with respect to the first medium. Equation (3.1) is called Snell's law of refraction, n_{21} is a characteristic of the pair of media (and also depends on the wavelength of light), but is independent of the angle of incidence.

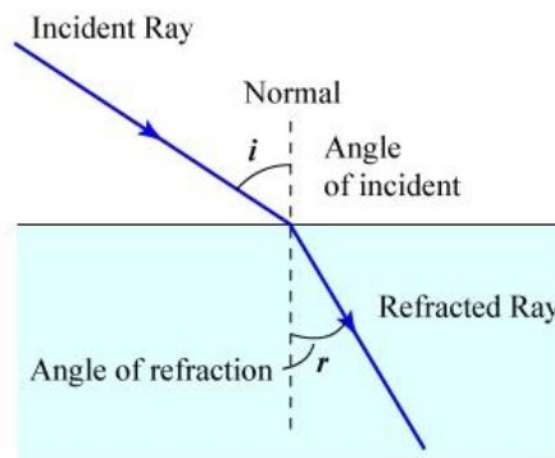


Figure 3.1 Phenomenon of refraction

3.3 Negative Refraction

Negative Refraction [37, 38] is an electromagnetic phenomenon where light rays are reflected at an interface in the reverse direction to that normally expected. Such effect can be obtained using a metamaterial which has been designed to achieve negative value for both electric (ϵ) and magnetic (μ) permeability [40, 41]. Such type of materials can be assigned as negative refractive materials (NRM) [39] and sometimes called double negative materials. Negative refraction occurs at interface between materials one has simply positive phase velocity (positive refractive index) and the other has the negative phase velocity (negative refractive index [37, 38]). Group velocity and phase velocity are in opposite direction due to negative refraction. The wave-vector k in an isotropic NRM points opposite to the direction of the pointing vector $S = E \times H$ which gives the negative refraction effect. Thus it is clear that the phase velocity $v_\phi = \frac{\omega}{k}$

is negative. The group velocity, which is defined by $\vec{v}_g = \frac{\partial \omega}{\partial \vec{k}}$ is along the direction of the pointing vector and oriented opposite to the phase velocity. The group velocity in a homogeneous isotropic medium can be expressed as:

$$\vec{v}_g = \pm \frac{\partial \omega}{\partial \vec{k}} \quad (3.2)$$

Where, $p = \pm 1$, depending on the choice of sign of the square root as the frequency does not depend on the direction due to isotropy. This means that the group velocity can only be parallel, (in a positive medium) or anti-parallel (in an NRM) to the phase velocity. The negative refraction depends upon some effects such as modified Snell's law of refraction, Reversed Doppler Effect and Cerenkov radiation.

3.3.1 Modified Snell's law of refraction

The refraction of radiation at the interface of a positive medium and a negative medium has been one of the most important parameters for image processing in photonic crystal. Consider the electromagnetic plane wave incident on an NRM from a positive medium with a wave vector $(k_x, 0, k_{z+})$. The continuity of the fields and Maxwell's equations require the transmitted wave-vector to be $(k_x, 0, k_{z-})$. Pointing vector is oriented exactly opposite to the phase vector \vec{k} , in the NRM, and we realize that the ray representing the energy flow corresponding to the refracted wave should lie on the other side of the normal as shown in figure 3.2(a). This negative angle can also be written as from Snell's law,

$$n_+ \sin \theta_+ = n_- \sin \theta_- \quad \text{Where, } n_- < 0 \Rightarrow \theta_- < 0. \quad (3.3)$$

The modification of Snell's law is counter to a very fundamental concept in optics of isotropic media that, depending on how dense the second medium is, the refracted wave can bend as close to the normal as possible, but never cross it. In this case, the refracted beam actually emerges on the other side of the normal. The angle of the reflected beam remains unaffected. Figure 3.2 (b) shows the negative refraction through a prism which was used in the experiments.

A flat slab of an NRM with $n = -1$ can focus a source as shown in figure 3.2 (c). This lens is different from the usual optical lens with curved surfaces in that it does not focus rays from

infinity to a point. These rays would simply pass through unaffected, rays emanating from a point source located at a distance d_1 on one side of the slab would be refocused to a point at a distance d_2 on the other side, provided that $d_1 + d_2 = d$, where d is the thickness of the slab. In fact, the total phase shift accumulated by any wave in going from the source point to the image point is zero as a consequence of the negative phase vector inside the NRM. This is in contrast to the phase corrections that are made to different rays in a conventional lens. Hence a convex lens causes a plane wave to diverge while a concave lens causes the plane wave to become convergent.

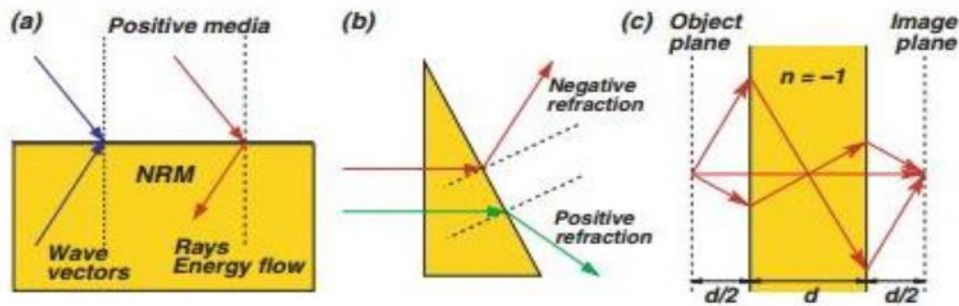


Figure3.2 (a) Schematic description of the negative refraction at an interface between a positive medium and a negative medium, the energy flow and the phase vectors are in opposite directions in the NRM. (b) The negative refraction effect through a prism. (c) Flat slab of NRM that can focus a point source from one side of the slab to the other side. Source (www.iopscience.iop.org)

3.3.2The reversed Doppler shift

Assume a moving source emitting radiation at a frequency ω in an NRM with a velocity v with respect to the medium. The frequency measured by a detector in the frame of the NRM is

$$\omega' = \Upsilon (\omega + k \cdot v) \quad (3.4)$$

Where $\Upsilon = (1 - v^2/c^2)^{-1/2}$ is the relativistic factor. $|k| = n\omega/c$, for emission along the direction of the motion of the source in the NRM (with $n = -1$)

$$\omega' = \Upsilon (\omega - \omega v/c) \quad (3.5)$$

The frequency measured by a detector would be smaller when the source is moving towards it, this is counter to the frequency increase that we would get in a normal medium. Again it is the reversed phase vector in NRMs that is responsible for this reversed Doppler shift.

3.4 Negative Refraction Using Photonic Crystals

It is diffractive in nature, one may often consider the electromagnetic waves in a photonic crystal as waves with new dispersion relations, $\omega_n(k)$, where n is the band index and k is the wave vector in the first Brillouin Zone. For a 3-D or 2-D photonic crystal, the direction of the energy flux is determined by group velocity, although it might not be true for 1-D photonic crystal. If the dispersion is isotropic, the condition $q \cdot d\omega_n(q)/dq < 0$, where q is the wave vector measured from a local extreme, must be satisfied for left handed behaviour [42]. This condition also allows the occurrence of negative at the interface of air and photonic crystal as well as the imaging effect with flat photonic slab [43,].

3.5 Negative Effective Index

In optics, the refractive index of a material is theoretically taken as a measure of the ‘optical density’ and it is defined in a medium as the ratio of speed of refracted light in vacuum to its speed in medium.

$$n = \frac{c}{v} \quad (3.6)$$

n = refractive index

c = speed of light in vacuum/air

v = speed of light in medium

The principle of refraction can be applied to all electromagnetic waves and not only for visible light. Every material, including air, has an index of refraction:

$$\frac{\sin \theta_1}{\sin \theta_2} = \frac{v_2}{v_1} \quad (3.7)$$

When an electromagnetic wave traverses the interface from a material with refractive index n_1 to another material with refractive index n_2 , the change in the direction of its trajectory can be determined from the ratio of refractive indices n_2/n_1 given by Snell's Law (figure 3.3).

$$n_1 \sin \theta_1 = n_2 \sin \theta_2 \quad (3.8)$$

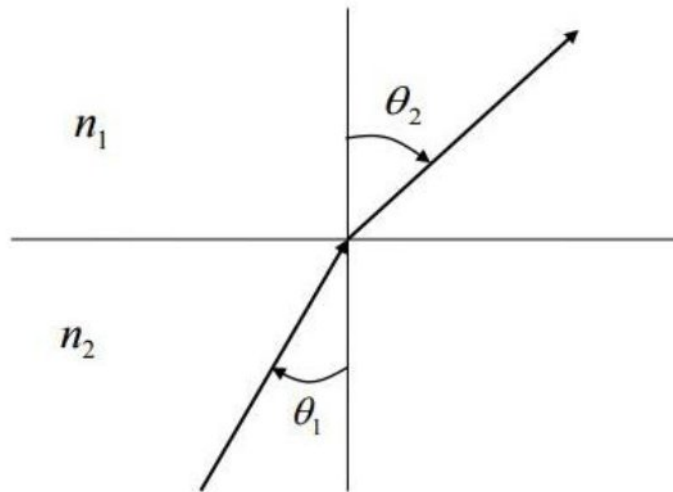


Figure 3.3 Principle of refraction by Snell's law.

(Source: www.study.com)

To apply Snell's Law, consider an interface between two materials and an imaginary line that runs perpendicular to the interface (the surface normal). The angles in Snell's Law are measured with respect to the surface normal. Maxwell's equation relates the permittivity and the permeability to the refractive index as follows:

$$n = \sqrt{\epsilon \mu} \quad (3.9)$$

The sign of the index is usually taken as positive. The Veselago showed that if a medium has both negative permittivity and negative permeability, this convention must be reversed: we must choose the negative sign of the square root. That mean, as Veselago hypothesized, a material with a negative refractive index could exist without violating any of the laws of physics. He also predicted that this remarkable material would exhibit a wide variety of new optical phenomena.

When the refractive index is negative, the phase velocity is given by c/n is negative and the wave travels backwards towards the source. The phase velocity determines the rate at which the peaks of a wave pass a given point in a given time. But this is not the most relevant definition of a

wave's velocity: we can also define the group, energy, signal and front velocities and these generally differ from the phase velocity.

When the refractive index of a material does not vary with the wavelength of light that travels through it, then all of the velocity definitions above are the same and we can intuitively use the index as a measure of the wave's velocity. When a material is dispersive, index that varies with wavelength then the various velocities are different. As Veselago showed, the phase and energy velocities are opposite in negative index materials. Negative refraction of waves propagating from one medium to another is a phenomenon where the light is refracted in a way to propagate along the same side as the incident light with respect to the normal of the interface, contrary to the normal light refractions as shown in figure 3.4.

A negative index of refraction would allow a flat slab of a material to behave as a lens. There are two types of negative refraction. The first type has simultaneous negative permittivity and negative permeability and the other type arises from beam steering phenomena in photonic crystals where we can get a negative refraction of the directions of the group velocities at the interfaces

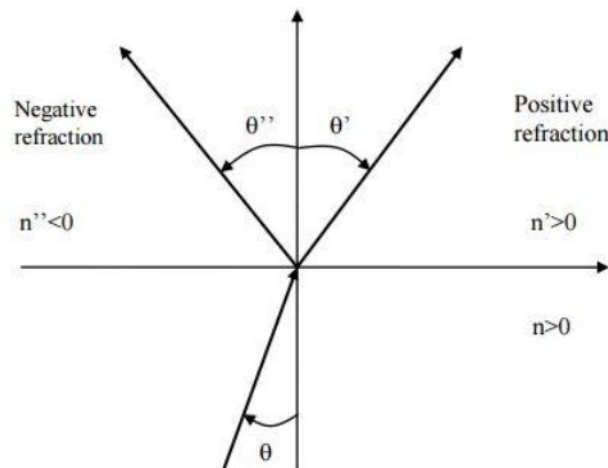


Figure3 .4 Negative and positive refraction

(Source: www.trnmag.com)

Negative refraction leads to a variety of interesting phenomena and potential applications. One of the most interesting applications is the superlens. Pendry suggested that a negative index material slab could make a superlens with a resolution far beyond the diffraction limit that is inherent in

the conventional far-field lens. For the near-field case, a negative index material slab can amplify the evanescent wave components to form a high-resolution image.

3.6 Sub Wavelength Imaging

One of the properties of negative index materials is their ability to focus light. Conventional lenses are convex and have a converging effect on light rays. The resolution of a conventional (convex) lens is always limited by the wavelength of the light. A light beam cannot be focused to a spot with a diameter smaller than about half of the wavelength of the light [42]. In 1968, Veselago [44] has shown theoretically that a convex lens made of a negative index material would lead to a divergent light, and that a concave lens made of negative index material would lead to a convergent light [44]. This behavior is thus opposite to the behavior observed for conventional convex and concave lenses made of positive index materials. Veselago also noted that a flat plate of thickness T made of negative index material with $n = -1$ and located in vacuum can focus radiation from a point source P positioned at a distance $D < T$ from one side of the plate to the point P located at a distance $T - D$ from the other side of the plate [44]. When the source is closer to the slab, or the slab becomes thicker, the distance of the refocus will be increased. Veselago also remarked that the flat plate, unlike a conventional lens, will not focus at a point a beam of rays coming from infinity (figure 3.5) [44].

In 1978, Silin showed that plane-parallel lenses can be constructed on the basis of media with negative dispersion [45]. In 2000, Pendry pointed out that flat slab of negative index material with $n = -1$ and surrounded by vacuum makes perfect lenses or superlenses since both propagating and evanescent waves contribute to the resolution of the image [42]. These lenses are just predicted to have sub-wavelength resolution better than the diffraction limit.

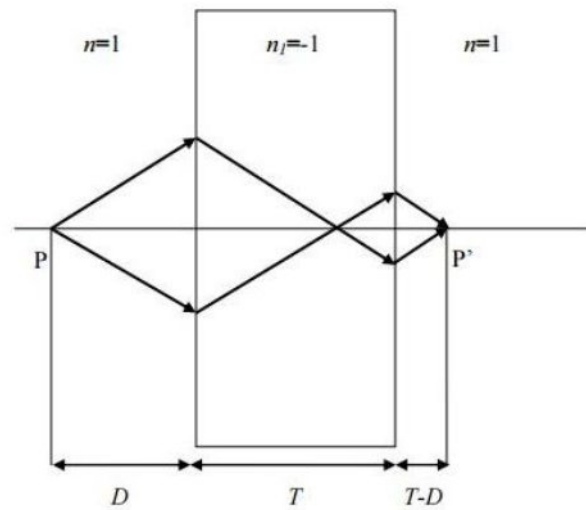


Figure 3.5 Imaging by a flat slab of thickness T of negative index material with $n_1 = -1$ and surrounded by vacuum. A point source P is positioned at a distance D from the left surface of the slab. A "perfect" image of the source can be observed at the point P' , located at a distance $T-D$ from the right surface of the slab.

3.7 Equal Frequency Contour

An essential tool for analyzing the conducting properties of a PhC is the equal-frequency surface (EFS) method [48-52]. The gradient of the EFS plays a major role in determining the group velocity direction, and the propagation direction of the photons in the PhC. EFS can be obtained by a numerical calculation employing a plane wave expansion methodology

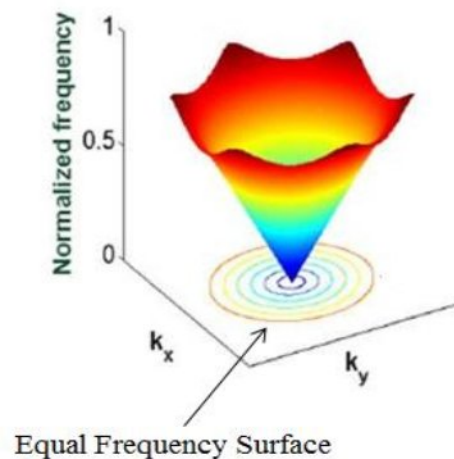


Figure 3.6 Equal frequency surfaces (EFSs) of a homogenous dielectric medium

(Source: cdn.intechopen.com/pdfs-wm/48056.pdf)

If the dielectric contrast of the PhC is large, then a large number of plane waves is required to obtain EFSs with good accuracy. Dispersion properties such as those of a superprism and beam splitting are normally well pronounced in PhCs with a small dielectric modulation [53–56] for which the requirement on the large number of plane waves to obtain EFS. The EFS analyzed by full zone analysis for second band in band gap structure. The frequency at which $n_{\text{eff}} = -1$ [46] has been analyzed at that point where EFS started become circular as shown in figure 3.6.

CHAPTER 4

ENHANCED IMAGE RESOLUTION IN PHOTONIC CRYSTAL STRUCTURE BY MODIFICATION OF THE SURFACE STRUCTURE AND ITS APPLICATION AS A SENSOR

4.1 Introduction

Flat slab of left handed materials [42] with an index $n = -1$ can serve as a perfect lens [42] to break the limit of diffraction due to amplifying evanescent waves. The negative index materials have many exotic electromagnetic properties, such as negative refraction [37, 38] reversed Doppler shift and reversed Cerenkov radiation. In the microwave regime, metamaterials (artificially structured periodic materials) have been proved to superlenses [42]. There are two types of imaging behaviors based on negative refraction for PhCs. One is a restricted near-field imaging, which does not need an isotropic effective negative index. The other is an unrestricted far-field imaging, which can provide an isotropic effective refractive index $n_{\text{eff}} = -1$ [46]. In 2000 this has been shown theoretically that photonic crystal, periodic dielectric composite structures with an electric permittivity $\epsilon > 0$ and a magnetic permittivity $\mu = -1$ at the frequency near the band gap behaves as if they have effective negative refractive index [47]. By analyzing the equi-frequency surface contours (EFS) [48-52], frequency at which the effective refractive index of photonic crystal is negative can be obtained where wave vector of incident wave and the group velocity of transmitted waves turn into opposite directions. Imaging effects have been proved experimentally as well as theoretically in hexagon lattice and square lattice. Many methods have been proposed to improve the image quality of the photonic crystal.

In this chapter, 2-D photonic crystal with enhanced image resolution by modification of surface structure has been proposed.

4.2 DesignParameters

The 2-D photonic crystal slab structure composed of hexagonal lattice of air holes in silicon ($\epsilon = 12$) has been considered as shown in figure 4.1. The radius (r) of air holes and thickness of slab (w) has been taken as ' $r = 0.35a$ ' and ' $w = 6.88a$ ' respectively, Where ' a ' is lattice constant. The PhC slab structure consists of 41 columns of air holes in X direction & 7 columns of air holes in Z direction. The plane wave expansion method has been used to obtain the band diagram& equi frequency contours of 2-D photonic crystal structure. The structure has an effective isotropic

index of $n_{\text{eff}} = -1$ at $\omega = 0.2908(2\pi c/a)$ for TM polarization analyzed from band diagram with light line and equal frequency contour as shown in figures 4.2 (a) and (b) respectively. Similar analysis has been done for TE polarization, but no such effect is observed. Hence, further analysis has been done for TM polarization only.

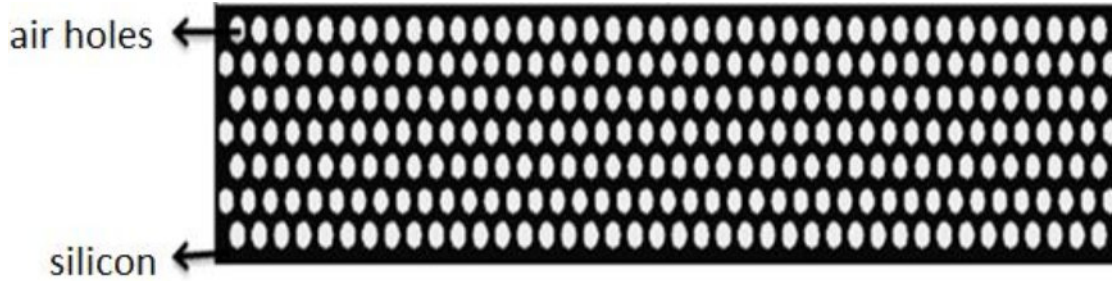


Figure – 4.1 PhC structure compose of air holes of radius ' $r = 0.35a$ ' in silicon

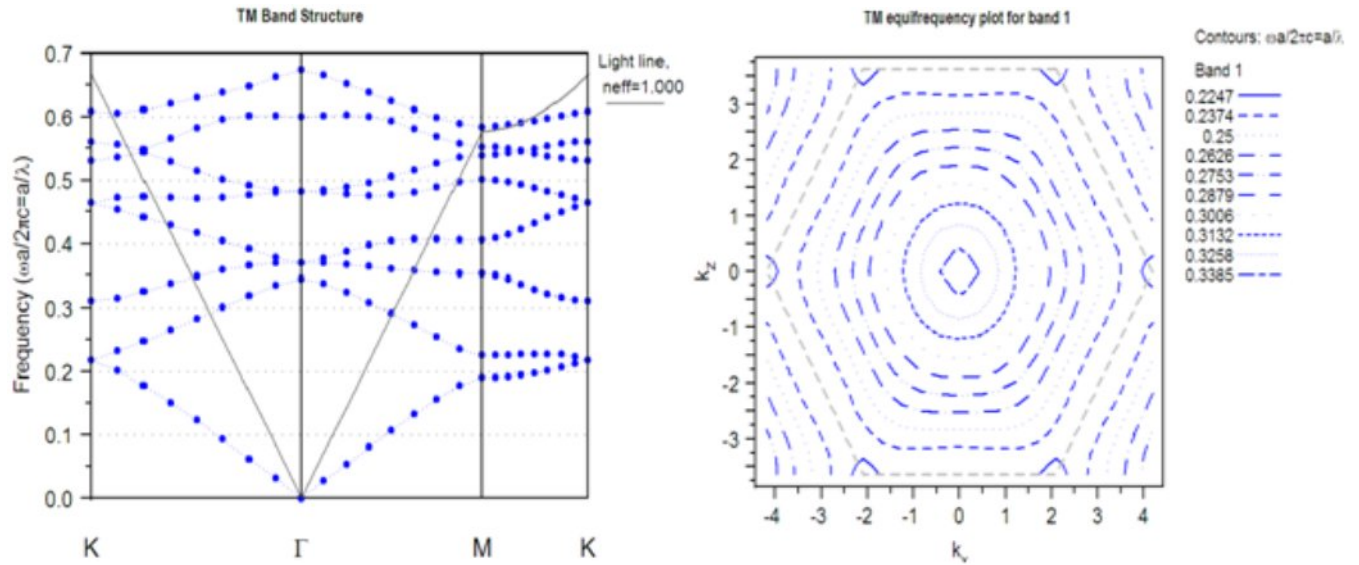


Figure-4.2 (a) band gap of PhC structure compose of air holes of radius ' $r = 0.35a$ ' with light line for TM polarization. (b) Several equal frequency contour of the second band at the TM mode in the first Brillouin zone

4.3 Numerical Analysis

The considered structure has been analyzed using the finite difference time domain (FDTD) method having perfectly matched layer for image resolution. A continuous wave point source having normalized frequency of $0.2908 (2\pi c/a)$ is placed at $(0, -6.86a)$ under the photonic crystal slab structure. The distance between source and PhC slab has been taken as $3.42a$ which is close to half of thickness of PhC slab ($3.44a$), so as to obtain a good quality image. If image is formed at a distance of double the thickness of PhC slab from source, slab behaves like superlens and negative refraction occurs. The Full width at half maxima (FWHM) obtained from the normalized intensity as shown in figure 4.3 (b) has been obtained to be 0.597λ . The FWHM value is greater than 0.5λ and considered to be poor.

In order to improve the resolution, the surface structure and the radius of air holes in the both the top and bottom row have been modified as shown in figure 4.4(a). The bottom layer of air holes consists of two semicircles of radius r_1 . Radius of top layer and bottom layer of air holes has been varied from $0.30a$ to $0.45a$ where the position of source $(0, -6.86a)$ has been constant. The distance between two semicircles is denoted by 'd' as shown in figure 4.4(b). Distance between two semicircles has been also varied from $0.41a$ to $0.44a$. Figure 4.5 clearly shows that when ' $r_1 = 0.41a$ ' and the distance between two semicircles is $0.43a$, then better image quality has been obtained. The FWHM has obtained to be 0.311λ that indicates better image quality. Thus the optimized parameters of the structure are ' $r_1 = 0.41a$ ' and ' $d = 0.43a$ '.

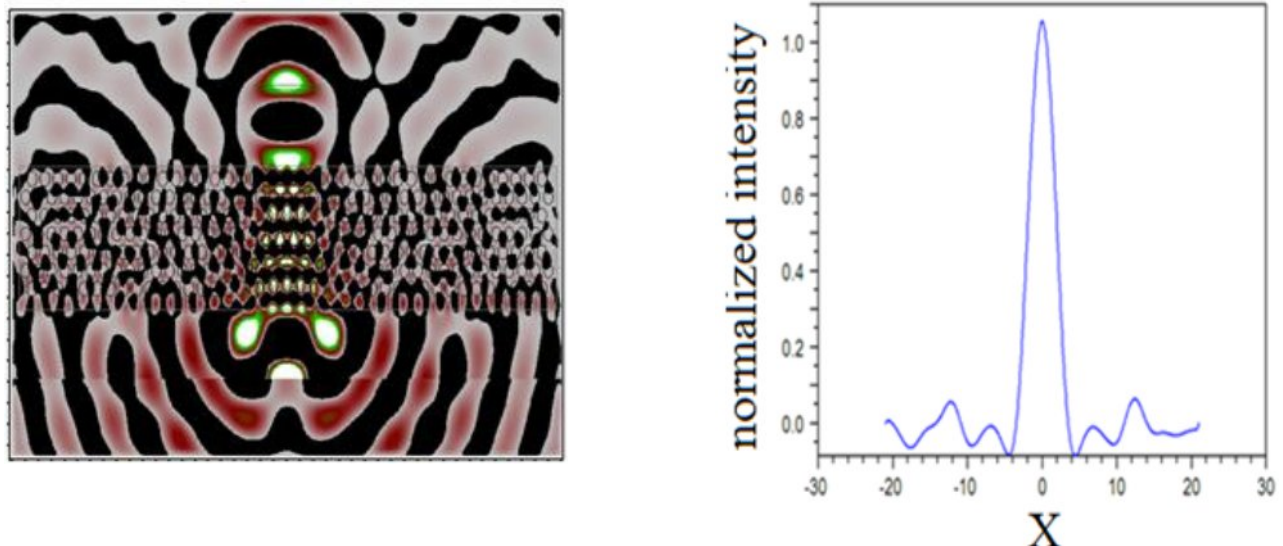


Figure – 4.3 Image processing and field distribution across image center along X-direction

The FWHM of the modified slab has been reduced by 47% as compared to the FWHM of the original slab. This indicates better image quality.

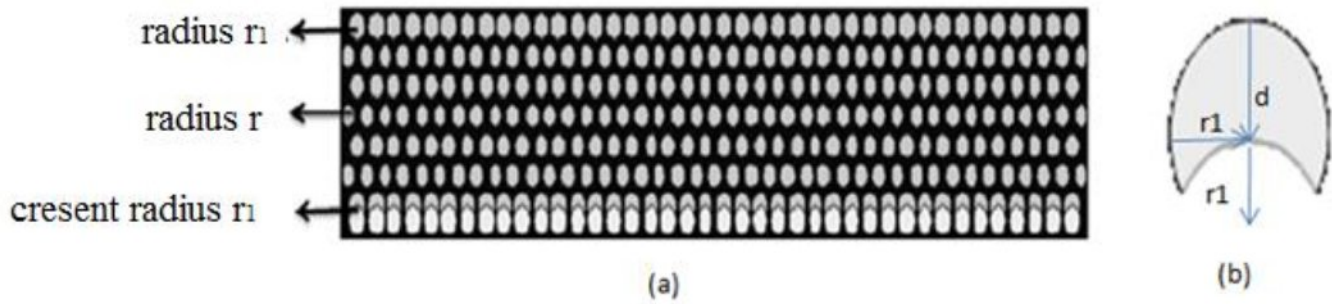


Figure-4.4(a) modified photonic crystal structure with radius ' $r = 0.35a$ ' and ' $r_1 = 0.41 a$ '; (b) radius of outer semicircle and semi circle is r_1 and distance between two semicircles is d .

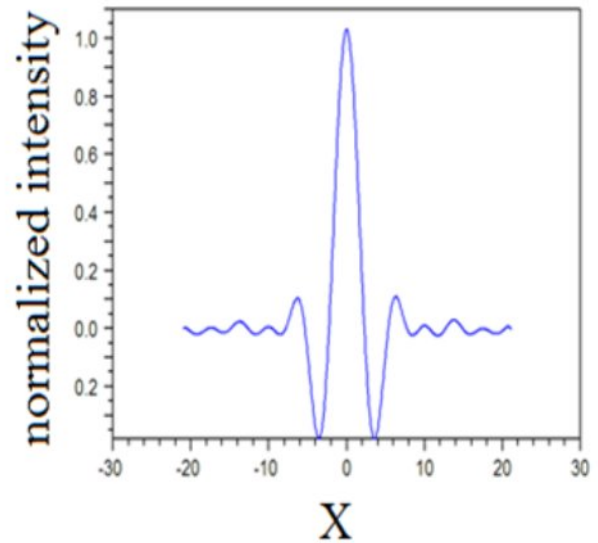
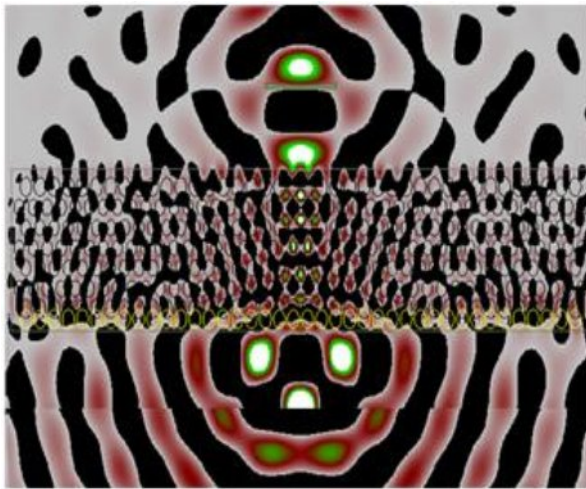


Figure-4.5 Image processing and field distribution across image center along X- direction of modified photonic crystal structure

4.4 Application of proposed structure as a sensor

The optimized structure can be used as a sensor. For the operation of proposed structure as a sensor the top and the bottom layers of air holes have been filled with various blood constituents as mentioned in table 1. After filling the top and bottom air holes with specific blood constituents, the image has been formed at a certain distance. The variations of intensity, peak and FWHM with respect to refractive index have been tabulated in table1 and table 2

corresponding to the proposed blood constituents. Normalized intensity graphs for the all blood constituents are shown in figure 4.6 (a)-4.6 (h)

The graphs of intensity and FWHM with respect to refractive index have been plotted. It has been observed from figure 4.7 that intensity increases with increases the refractive index of blood constituents which filled in top and bottom layer of holes, further observed from figure 4.8 FWHM decreases with increase the refractive index and hence image becomes more focused. This Variation in the peak value of intensity and FWHM, hence the image quality can be used for sensing the various blood constituents.

TABLE-1
Blood constituents filled in top layer

BLOOD CONSTITUENTS	REF. INDEX	INTENSITY	PEAK	FWHM
cytop	1.34	0.651	1.02	0.325λ
blood plasma	1.35	0.652	1.02	0.323λ
ethanol	1.36	0.653	1.02	0.319λ
hemoglobin	1.38	0.658	1.02	0.317λ
glucose	1.4	0.663	1.01	0.316λ
Sylgard 184	1.43	0.668	1.00	0.314λ
Biotin-streptavidin	1.45	0.672	1.00	0.311λ
bovine	1.47	0.676	1.00	0.309λ

The results which tabulated in table 1 shows that improved FWHM is achieved at refractive index ($n = 1.47$) is 0.309 λ . This indicates the better image quality of proposed structure with filled constituents in top layer. We have calculated the sensitivity of intensity with respect to refractive index. The sensitivity of intensity is defined as ratio of derivative of intensity and derivative of refractive index.

TABLE-2

Blood constituents filled in bottom layer

BLOOD CONSTITUENTS	REF. INDEX	INTENSITY	PEAK	FWHM
cytop	1.34	0.600	1.16	0.368λ
blood plasma	1.35	0.600	1.17	0.365λ
ethanol	1.36	0.600	1.16	0.366λ
hemoglobin	1.38	0.607	1.16	0.365λ
glucose	1.4	0.610	1.15	0.365λ
Sylgard 184	1.43	0.607	1.14	0.365λ
Biotin-streptavidin	1.45	0.608	1.12	0.371λ
Bovine	1.47	0.606	1.12	0.371λ

$$S(\Delta I, \Delta n) = \frac{\frac{\partial I}{\partial n}}{\frac{\partial I}{\partial n}} \quad (4.1)$$

$$= \frac{\frac{\partial I}{\partial n}}{\frac{\partial I}{\partial n}}$$

$$= 0.25$$

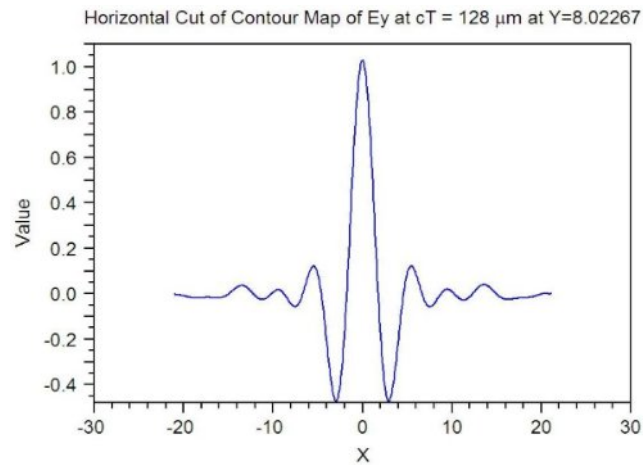
Similarly sensitivity of FWHM with respect to refractive index has been calculated.

$$S(\Delta F, \Delta n) = \frac{\frac{\partial F}{\partial n}}{\frac{\partial F}{\partial n}} \quad (4.2)$$

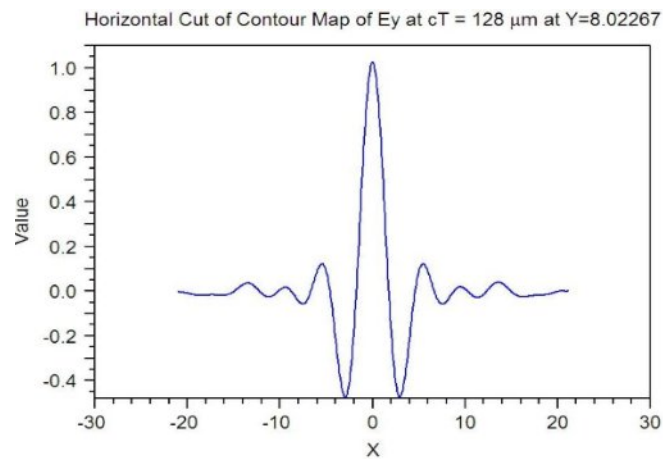
$$= \frac{\frac{\partial F}{\partial n}}{\frac{\partial F}{\partial n}}$$

$$= 0.1$$

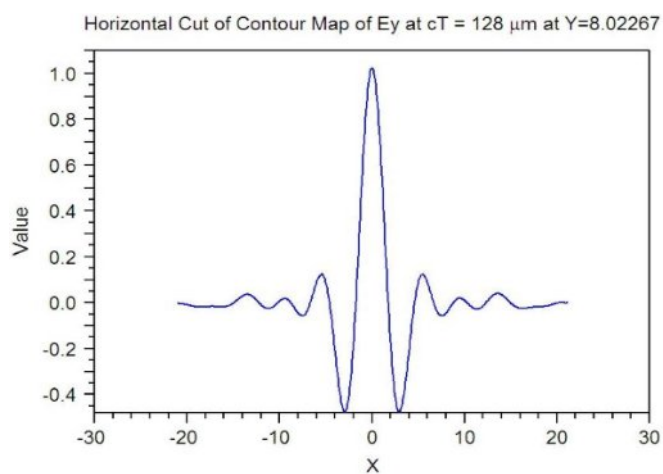
The Proposed structure can behave negative refractive index sensor with $S(\Delta I, \Delta n) = 0.25$ and $S(\Delta F, \Delta n) = 0.1$



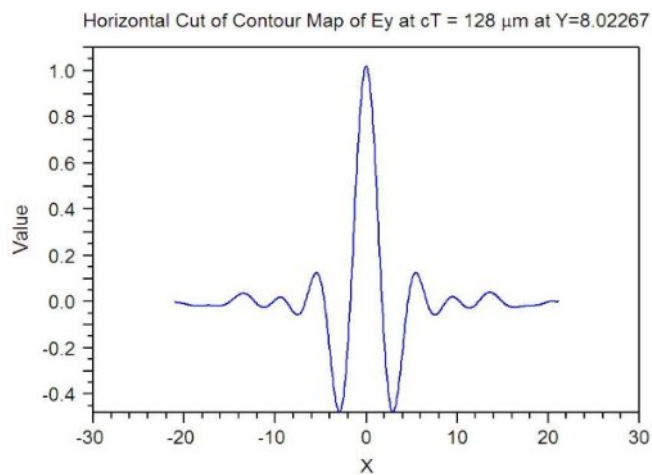
(a) Cyotop



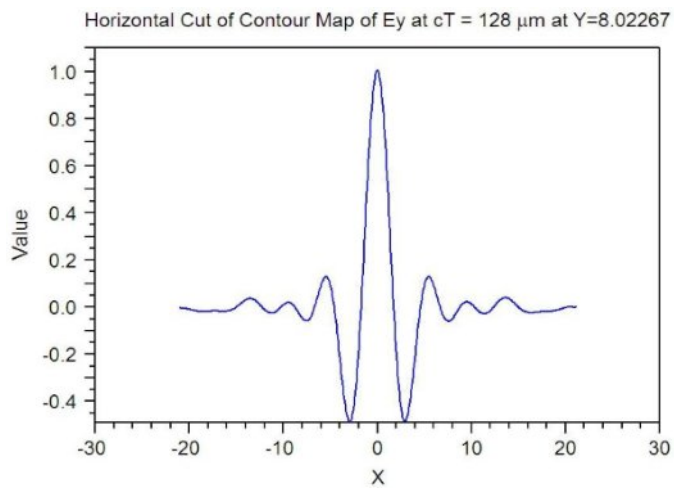
(b) Blood Plasma



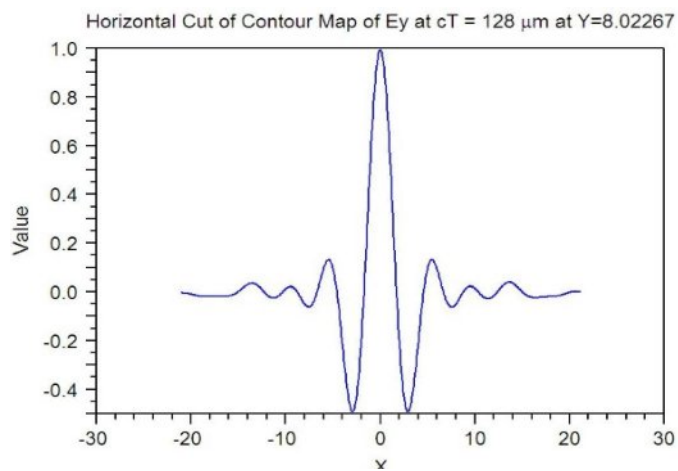
(c) Ethanol



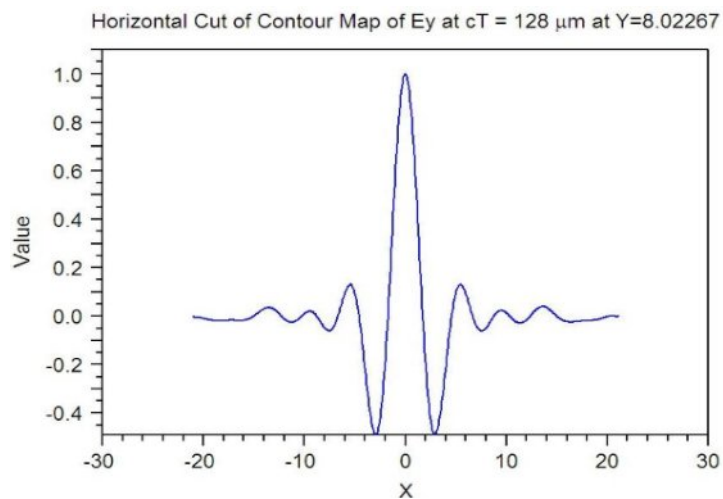
(d) Hemoglobin



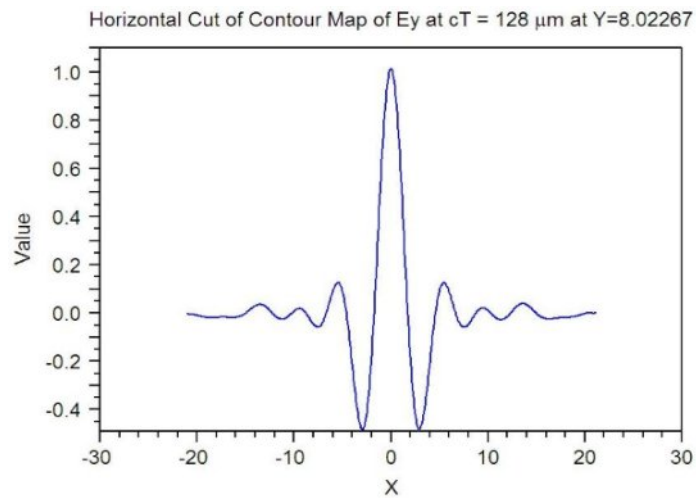
(e) Glucose



(f) Sylgard



(g) Biotin



(h) Bovine

Figure 4.6 Peak graphs of all blood constituents filled in top layer

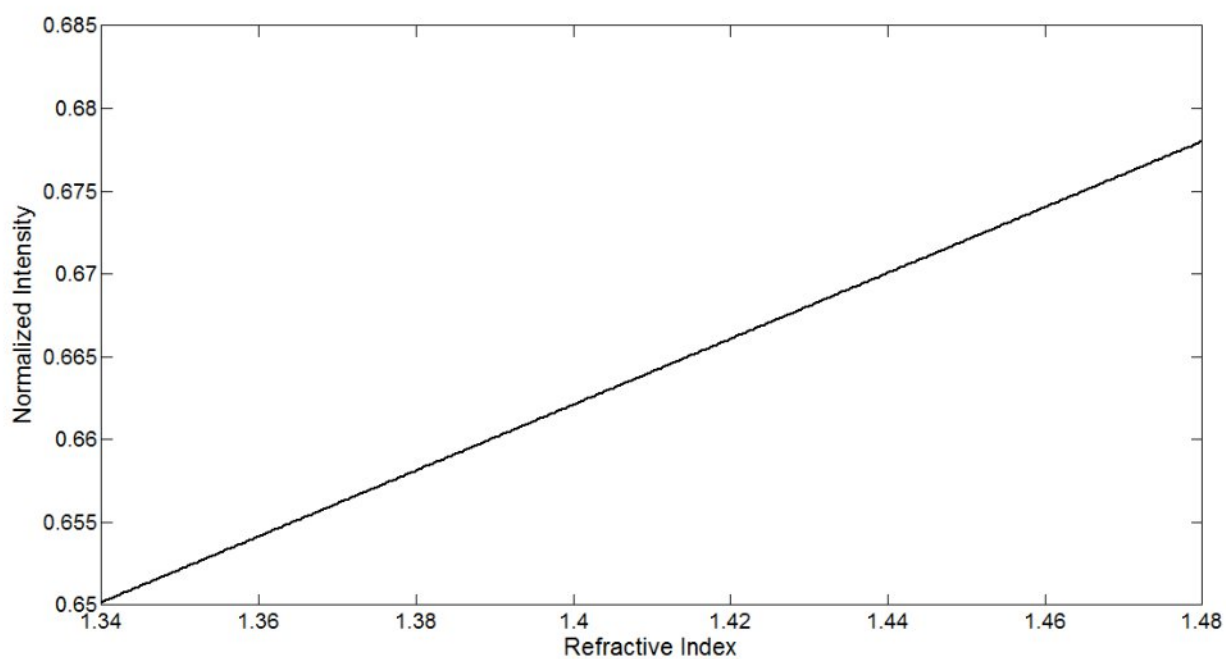


Figure 4.7 Intensity curve of different type of blood constituents, intensity peak increased when refractive index increased.

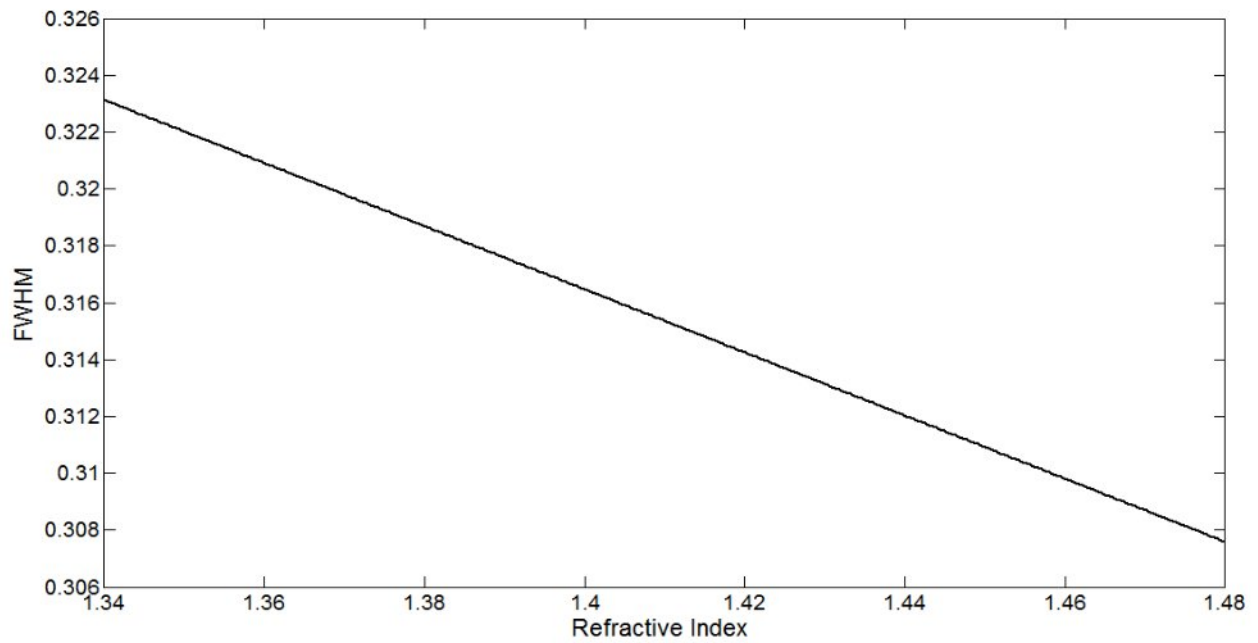


Figure 4.8 FWHM curve of different type of blood constituents, FWHM decreased when refractive index increased

4.5 Conclusion

The enhanced image resolution by modification in the photonic crystal structure has been successfully obtained. The structure has been modified by perturbing the radii of the top and bottom layers of the photonic crystal structure, which led to the better image resolution at a normalized frequency of $0.2908a$ with $\text{FWHM} = 0.311\lambda$.

CHAPTER 5

CONCLUSION AND FUTURE SCOPE

5.1 Conclusion

The enhanced image resolution by modification in the photonic crystal structure has been successfully proposed. The structure has been modified by perturbing the radii of the top and bottom layers of the photonic crystal structure. The modified structure has an effective isotropic refractive index of $n_{\text{eff}} = -1$ for TM polarization analyzed using equal frequency contours as calculated by plane wave expansion method. The image quality has been improved with full width at half maximum (FWHM) of 0.311λ . The FWHM of the image focused by changed PhC slab has been less ephemeral than the original PhC slab when analyzed by using different type of blood constituents filled in top layer. The proposed structure has been used as a refractive index sensor for sensing various blood constituents. The structure is sensitive to intensity peak and full width at half maxima (FWHM) of different type of blood constituents.

5.2 Future Scope

Due to the ability of subwavelength imaging, negative refractive lenses can revolutionize medical science. Being used as a biomedical sensor and/or an imaging device, they can be very helpful in medical diagnosis.

The proposed structure can be designed in silicon on insulator (SOI) structure to enhance the image resolution. Silicon on insulator is the technology which uses layered silicon –insulator-silicon- substrate in place of a conventional silicon substrate. The crystalline silicon layer is sandwiched between the hidden insulator (Silicon oxide, Sapphire etc.) and the top cladding of air (or Silicon oxide or any other low refractive index material). This enables propagation of electromagnetic waves in the waveguides on the basis of total internal reflection.

The proposed structure (based on air holes in silicon) works for TM mode only. However, by suitably modifying the geometrical parameters one can also develop a polarization independent structure which works efficiently for both - TE and TM polarizations.

The image resolution of proposed structure depends upon the shape of holes, size of holes etc. The image resolution can be enhanced by use of elliptical holes in place of the circular ones. This is due to the fact that elliptical holes will have higher filling factor than the circular holes. Hence the focus can be sharper and resolution can be better.

The air holes of the structure can be infiltrated by liquid crystal to enhance image resolution. Liquid crystals have properties between those of a conventional liquid and a solid crystal. A liquid crystal may flow like a liquid, but its molecules are oriented in a crystal like structure. By the infiltration the light focusing ability of the structure can be improved and an enhanced image can be obtained.

Moreover, the proposed structure can also be used in combination with a metal grating to improve image resolution. It can be used to analyze the imaging effect of high-order diffracted waves, which carry a lot of high-frequencies information excited by the subwavelength metallic grating.

References:

- [1] Yablonovitch, E.(1987).Inhibited spontaneous emission on solid-state physics and electronics”, Physics Review Letters, 58(20), 2059-2062.
- [2] John, S. (1987). Strong localization of photons in certain disordered dielectric superlattices”, Physics Review Letters,, 58(23), 2486-2489.
- [3]Ma, Z, & Ogusu, K. (2011). Channel drop filters using photonic crystal fabry-perot resonators”, Optics Communications,, 284(5), 1192-1196.
- [4] Mohmoud, M. Y, Bassou, Z. M, Taalbi, A, & Chekroun, Z. M. (2012). Optical channel drop filters based on photonic crystal ring resonators”, Optics Communications,, 285(1), 368-372.
- [5] Rawal, S, & Sinha, R. K. (2009). Design, analysis and optimization of silicon-on-insulator photonic crystal dual band wavelength demultiplexer”, Optics Communications, ,282(19), 3889-3894.
- [6] Benisty, H, Cambournac, C, Laere, F. V, & Thourhout, D. V. (2010). Photonic crystal demultiplexer with improved crosstalk by second-order cavity filtering”, Journal of Lightwave Technology, , 28(8), 1201-1208.
- [7] Wang, Q, Cui, Y, Zhang, H, Yan, C, & Zhang, L. (2010). The position independence of heterostructure coupled waveguides in photonic-crystal switch”, Optik Optics, , 121(8),684-688
- [8] Moghaddam, M. K, Attari, A. R, & Mirsalehi, M. M. (2010). Improved photonic crystal directional coupler with short length”, Photonics and Nanostructures-Fundamentals and Applications, , 8(1), 47-53.

[9] Gannat, G. A, Pinto, D, & Obayya, S. S. A. (2009). New configuration for optical waveguide power splitters", IET Optoelectronics, , 3(2), 105-111.

[10] Abdel Malek F ((2011). Design of a novel left-handed photonic crystal sensor operating in aqueous environment", IEEE Photonics Technology Letters, , 23(3), 188-190.

[11] Olyaei, S, & Dehghani, A. A. (2012). High resolution and wide dynamic range pressure sensor based on two-dimensional photonic crystal", Photonic Sensors, , 2(1), 92-96.

[12] Bruyant, A, Lerondel, G, Reece, P. J, & Gal, M. (2003). All silicon omnidirectional mirrors based on one-dimensional photonic crystals", Applied Physics Letters,, 82(19),3227-3229.

[13] Li, Y, Xiang, Y, Wen, S, Yong, J, & Fan, D. (2011). Tunable terahertz mirror and multi channel terahertz filter based on one dimensional photonic crystals containing semiconductors", Journal of Applied Physics, , 110(7), 073111-073111.

[14] Chen, M. C, Luan, P. G, & Lee, C. T. (2003). Novel design of organic one-dimensional photonic crystal filter", in the Proceedings of the 5th IEEE International Conference on Lasers and Electro-Optics, , 2, 1-4.

[15] Nemec, H, Duvillaret, L, Garet, F, Kuzel, P, Xavier, P, Richard, J, & Raully, D. (2004). Thermally tunable filter for terahertz range based on a one-dimensional photonic crystal with a defect", Journal of Applied Physics, , 96(8), 4072-4075.

[16] Lee, H. Y, Cho, S. J, Nam, G. Y, Lee, W. H, Baba, T, Makino, H, Cho, M. W, & Yao, T.(2005). Multiple wavelength transmission filters based on Si-SiO₂ one dimensional photonic crystals", Journal of Applied Physics,, 97(10), 103111-103111.

[17] Lu, T. W, Chiu, L. H, Lin, P. T, & Lee, P. T. (2011). One-dimensional photonic crystal nanobeam lasers on a flexible substrate", Applied Physics Letters, , 99(7),071101-071101

- [18] Ogawa, S, Tomoda, K, & Noda, S. (2002). Effects of structural fluctuations on threedimensional photonic crystals operating at near-infrared wavelengths”, Journal of Applied Physics, , 91(1), 513-515.
- [19] Yang, Y. L, Hou, F. J, Wu, S. C, Huang, W. H, Lai, M. C, & Huang, Y. T. (2009). Fabrication and characterization of three dimensional all metallic photonic crystals for nearinfrared applications”, Applied Physics Letters, , 94(4), 041122-041122.
- [20] Baohua, J, Buso, D, Jiafang, L, & Min, G. (2009). Active three dimensional photonic crystals with high third order nonlinearity in telecommunication”, in the Proceedings of the IEEE International Conference on Lasers and Electro Optics,, 1-2.
- [21] Deubel, M, Von Freymann, G, Wegener, M, Pereira, S, Busch, K, & Soukoulis, C. M.(2004). Direct laser writing of three dimensional photonic crystal templates for photonic bandgaps at telecommunication wavelengths”, in the Proceedings of the IEEE International Conference on Lasers and Electro Optics, , 1-3.
- [22] Ohkubo, H, Ohtera, Y, Kawakami, S, & Chiba, T. (2004). Transmission wavelength shift of +36 nm observed with Ta₂O₅-SiO₂ multichannel wavelength filters consisting of threedimensional photonic crystals”, IEEE Photonic Technology Letters, , 16(5), 1322-1324.
- [23] Liu, R. J, Li, Z. Y, Feng, Z. F, Cheng, B. Y, & Zhang, D. Z. (2008). Channel drop filters in three dimensional woodpile photonic crystals”, Journal of Applied Physics, , 103(9), 094514-094514
- [24] Taflov, A. & Hagness, S. C. 2005 Computational electrodynamics: the finite-difference time-domain method, 3rd edn. Boston: Artech House.
- [25] Joannopoulos, J. D. 2008 Photonic crystals: molding the flow of light, 2nd edn. Princeton: Princeton University Press.

- [26] Johnson, S. & Joannopoulos, J. 2001 Block-iterative frequency-domain methods for Maxwell's equations in a planewave basis. *Opt. Express* **8**, 173-190.
- [27] Yee, K. 1966 Numerical solution of initial boundary value problems involving Maxwell's equations in isotropic media. *IEEE Trans. Ant. Prop.* **14**, 302-307.
- [28] O. Painter, J. Vuckovic', and A. Scherer, Defect modes of a two-dimensional photonic crystal in an optically thin dielectric slab, Vol. 16, No. 2/February 1999/J. Opt. Soc. Am. B.
- [29] S. E. Dissanayake, K. A. I. L. Wijewardena Gamalath 2015, Point defects in GaAs photonic crystals, International Letters of Chemistry, Physics and Astronomy Online: 2015-01-04 ISSN: 2299-3843, Vol. 43, pp 91-102 doi:10.18052.
- [30] L. P. Bouckaert, * R. Smolucowski and E. Wigner, Theory of Brillouin Zones and Symmetry Properties of Wave Functions in Crystals, Physical Review, Vol. 50.
- [31] Ruei-Chang Lu, Yu-Lung Jang, Coupling Device with Resonant Cavities Based on Periodic Dielectric Waveguides, Optics and Photonics Journal, 2013, 3, 240-242
- [32] Yao Peijun *,1, Chen Xiyao, Chen Bo, Lu Yonghua, Wang Pei, Jiao Xiaojin, Ming Hai, Xie Jianping, Optical reflector and high Q filter based on two-dimensional photonic-crystal waveguide, Optics Communications 236 (2004) 101-107
- [33] C. Jamois, R.B. Wehrspohn, L.C. Andreani, C. Hermann, O. Hess, U. Gösele, Silicon-based two-dimensional photonic crystal waveguides, Photonics and Nanostructures – Fundamentals and Applications 1 (2003) 1-13
- [34] Steven G. Johnson, Pierre R. Villeneuve, Shanhui Fan, and J. D. Joannopoulos, Linear waveguides in photonic-crystal slabs, Physical Review, VOL. 62, Number 12

- [35] S Anantha Ramakrishna, Physics of negative refractive index materials, institute of physics publishing, doi:10.1088/0034-4885/68/2/R06
- [36] Henry Semat, Reflection and Refraction, Research Papers in Physics and Astronomy, 1-1-1958
- [37] Masaya Natomi, Negative Refraction in Photonic Crystal, optical and quantum electronics, 34: 133-143, 2002
- [38] Liyong Jiang , Hong Wu, Xiangyin Li, Alternative approach to realize all-angle negative refraction and far-field imaging effects via two-dimensional all-solid photonic crystals, Optics Communications 285 (2012) 2462–2465
- [39] Victor Veselago, Negative Refractive Index Materials, Journal of Computational and Theoretical Nanoscience Vol.3, 1–30, 2006
- [40] R.A. Shelby, D.R. Smith, S. Schultz, Experimental verification of a negative index of refraction, Science 292 (2001) 77–79.
- [41] T. Koschny, M. Kafesaki, E.N. Economou, C.M. Soukoulis, Effective medium theory of left-hand materials, Phys. Rev. Lett. 93 (2004) 107402-1-4.
- [42] J.B. Pendry, "Negative Refraction Makes a Perfect Lens," Phys.Rev.Lett, Vol. 85, PP.3966-3969, 2000
- [43] P.V. Parimi, W.T.T. Lu, P. Vodo, S. Shridhar, Nature 426 402 (2003)
- [44] V. G. Veselago, "The electrodynamics of substances with, simultaneous negative values of μ and ϵ Sov. Phys. Usp. 10, 509-514 (1968)
- [45] R. A. Silin, "Possibility of creating plane-parallel lenses," Opt. Spektrosk. 44, 189-191 (1978)

- [46] X. Wang, Z.F. Ren, K. Kempa, Unrestricted superlensing in a triangular two-dimensional photonic crystal, *Opt. Express* 12 (2004) 2919.
- [47] C. Luo, S.G. Johnson, J.D. Joannopoulos, J.B. Pendry, All-angle negative refraction without negative effective index *Phys. Rev. B* 65 (2002) R 201104
- [48] R. Gajic, R. Meisels, F. Kuchar, K. Hingerl, Anomalous refractive effects in honeycomb lattice photonic crystals formed by holographic lithography *Phys. Rev. B* 73 (2006) 165310.
- [49] J. Sun, Y.F. Shen, L.G. Wang, L.L. Sun, J. Wang, G.Z. Wang, Photon., Giant negative lateral shift and positive lateral shift due to leaky modes in a photonic band gap *Nanostruct.: Fundam. Appl.* 6 (2008) 219
- [50] Z.X. Tang, H. Zhang, Y.X. Ye, C.J. Zhao, R.W. Peng, S.C. Wen, D.Y. Fan, Improvement of the Focusing Resolution of Photonic Crystal Negative Refraction Imaging with a Hollow Component Structure, *Solid State Commun.* 141 (2007) 183.
- [51] S. Feng, Z.Y. Li, Z.F. Feng, K. Ren, B.Y. Cheng, D.Z. Zhang, J., Imaging Properties of a Rectangular-Lattice Metallic Photonic-Crystal Slab, *Appl. Phys.* 96 (2005) 063102
- [52] Z. Li, B. Liang, H. Guo, J. Chen, and S. Zhuang, “Negative refraction and birefringence in a two-dimensional flat perfect photonic crystal,” in *Optoelectronic Materials and Devices II*, vol. 6782 of *Proceedings of SPIE*, Wuhan, China, November 2007.
- [53] M. S. Li, S. T. Wu, and A.Yi-G. Fuh, “Superprism phenomenon based on holographic polymer dispersed liquid crystal films,” *Appl. Phys. Lett.* 88, 91109 (2006).
- [54] J. J. Baumberg, N. M. B. Perney, M. C. Netti, M. D. C. Charlton, M. Zoorob, and G. J. Parker, “Visible-wavelength super-refraction in photonic crystal superprisms,” *Appl. Phys. Lett.* 85, 354–356 (2004).

[55] G. Alagappan, X. W. Sun, P. Shum, and M. B. Yu, “Tunable superprism and polarization splitting in a liquid crystal infiltrated two-dimensional photonic crystal made of silicon oxynitride,” *Opt. Lett.* 31, 1109–1111 (2006).

[56] Y. J. Liu and X. W. Sun, “Electrically tunable twodimensional holographic photonic crystal fabricated by a single diffractive element,” *Appl. Phys. Lett.* 89, 171101 (2001).